Symplastic Solute Transport and Avocado Fruit Development: A Decline in Cytokinin/ABA Ratio is Related to Appearance of the Hass Small Fruit Variant

Clive S. Moore-Gordon[1], A. Keith Cowan[1], Isa Bertling[1], C. Edward J. Botha[2] and Robin H.M. Cross[3]

[1] Department of Horticultural Science, University of Natal, Pietermaritzburg 3209, South Africa
[2] Department of Botany, Schonland Botanical Laboratories, Rhodes University, Grahamstown 6140, South Africa
[3] Electron Microscopy Unit, Rhodes University, Grahamstown 6140, South Africa

Studies on the effect of fruit size on endogenous ABA and isopentenyladenine (iP) in developing avocado (Persea americana Mill. cv. Hass) fruit revealed that ABA content was negatively correlated with fruit size whilst the iP/ABA ratio showed a linear relationship with increasing size of fruit harvested 226 d after full bloom. The effect of this change in hormone balance on the relationship between symplastic solute transport and appearance of the small fruit variant was examined following manipulation of the endogenous cytokinin (CK)/ABA ratio. Application of ABA caused seed coat senescence and retarded fruit growth but these effects were absent in fruit treated with equal amounts of ABA plus iP. Thus, the underlying physiological mechanisms associated with ABA-induced retardation of Hass avocado fruit growth appeared to be inextricably linked to a decline in CK content and included: diminution of mesocarp and seed coat plasmodesmatal branching, gating of mesocarp and seed coat plasmodesmata by deposition of electron dense material in the neck region, abolishment of the electrochemical gradient between mesocarp and seed coat parenchyma, and arrest of cell-to-cell chemical communication.

Key words: Abscisic acid; Avocado {Persea americana); Hass small fruit variant; Isopentenyladenine; Plasmodesmata; Symplastic solute transport.

Abbreviations: CK, cytokinin; E_m, plasma membrane electrical potential; HMGR, 3-hydroxy-3-methylglutaryl coenzyme A reductase; iP, 6-(γ,γ -dimethylallylamino)-purine; IP_3/DAG, inositol triphosphate/diacyl glycerol; LYCH, Lucifer yellow-CH.

Hass avocado trees produce two distinct populations of fruit i.e. normal and small fruit (Zilkah and Klein 1987). The limiting parameter for growth of the small fruit variant appears to be cell number, and a reduction in cell number was shown to occur coincident with increased mesocarp ABA concentration and reduced 3-hydroxy-3-methylglutaryl coenzyme A reductase (HMGR) activity (Cowan et al. 1997). Since ABA-induced retardation of fruit growth, and inhibition of HMGR activity were negated by co-treatment with iP, a relationship between activity of HMGR and endogenous ABA and CK concentration in the metabolic control of Hass avocado fruit growth was suggested. Similarly, previous reports on phytohormone regulation of HMGR suggested that a change in hormone balance during development could impact on growth through modulation of HMGR (Bach and Lichtenthaler1983, Brooker and Russell 1979, Moore and Oishi 1994, Russell and Davidson 1982). While changes in amount of hormone result

from alterations in metabolism and/or transport, an increase in ABA or a decline in CK content may influence the supply of photoassimilate required for cell division and differentiation during avocado fruit ontogeny particularly as sucrose is thought to be involved in the induction of mitosis and protein synthesis (Koch 1996).

In developing fruit the bulk of carbon is derived from sugars, imported from source tissue (Ho 1988). In avocado, source tissues include photosynthetically active leaves and fruitlets (Coombe 1976, Thorne 1985, Blanke and Lenz 1989, Blanke and Whiley 1995). Additionally, stored tree reserves are mobilized during periods of organ growth to sustain development of these structures (Kozlowski 1992). Phloem is the most likely path of solute movement in dicotyledonous species and in developing fruit, phloem unloading occurs in the testa (Thorne 1985). However, in avocado the seed is exotestal (i.e. completely pachychalazal) and enclosed by a highly vascularized seedcoat (Steyn et al. 1993). It is the developing pachychalaza (i.e. the seed coat) that supplies photoassimilate, mineral nutrients and water to the developing fruit.

Two possible paths exist for the uptake of sugars from the seed coat in developing avocado fruit. Firstly, active transport via the plasma membrane and secondly, passive transport via plasmodesmata. Recent models of phloem unloading in developing fruits suggest that the passage of solute uptake by terminal sinks changes with development from symplastic to apoplastic (Patrick 1997). Unlike most other fruit, cell division in avocado occurs from fruit set to maturity which indicates a requirement for the maintenance of symplastic continuity throughout fruit growth and development (Ehlers and Kollmann 1996). Plasmodesmata are dynamic structures in which pore size, and hence size exclusion limit, is up-or down-regulated by processes involving callose deposition and removal from the annulus, and by structural modifications to the central lipoprotein core (Lucas et al. 1993, Morris 1996). A variety of agents are considered to be involved in the regulation of transport via plasmodesmata including: Ca^{2+} release, initiated by the inositol triphosphate-diacylglycerol (IP_3/DAG) second messenger system (Robards and Lucas 1990); phosphorylation of the callose synthesizing enzyme (Lucaset al. 1993); and, plant hormones (Morris 1996). Since many hormone responses appear to be mediated by the IP3/DAG signal transduction system it has been suggested that hormones like ABA, that are transported in the phloem, might act to modulate symplastic phloem loading and unloading by influencing protein phosphorylation (Morris 1996).

Casual observation has revealed that a characteristic of the Hass small fruit variant is early senescence of the seed coat. The question therefore arises: Are small fruit a consequence of early seed coat senescence, or is the abortion of seed coat function a response to some other factor induced by a reduction in HMGR activity and diminished cell division cycle activity?

It has been demonstrated that transgenic tobacco plants that constitutively express a yeast insoluble-acid invertase gene develop symptoms which are characteristic of the onset of early leaf senescence (Ding et al. 1993). Ultra-structural analysis of these transgenic plants revealed that development of secondary plasmodesmata was inhibited in the greenish-yellow sectors of affected leaves. Based on these observations, Ding et al. (1993) hypothesized that secondary plasmodesmata differ from primary plasmodesmata in being able to traffic regulatory molecules that are involved in the coordination of development and physiological function. In addition to these structural changes, biochemical and physiological studies showed accumulation of carbohydrates, a decline

in photosynthesis and increased respiration in leaves of transgenic tobacco expressing the yeast invertase gene (von Schaewen et al. 1990). Since these alterations in metabolism can also contribute to accelerated leaf senescence, it was further suggested that inhibition of secondary plasmodesmatal development may be the consequence of any change in carbon catabolism (Ding et al. 1993).

Carbohydrate availability affects carbohydrate allocation through altered gene expression and may therefore be crucial in the metabolic control of fruit growth. For example, sugar availability strongly affects cell differentiation and cell cycle activity in higher plants (Ballard and Wildman 1963, Webster and Henry 1987). Furthermore, carbohydrate supply is critical for kernel set in maize (Zinselmeier et al. 1995), fruit size of tomato (Klann et al.1996), and utilization of sugars in developing leaves, seed and fruit is strongly dependent on sucrose metabolizing enzymes (Klann et al. 1993, 1996, Miller and Chourey 1992,Ohyama et al. 1995) that are encoded by sugar responsive genes (Koch et al. 1992). This information suggests that availability of sugars and the composition thereof, are crucial for fruit development. Plant HMGR kinase, responsible for regulating the activity of HMGR, has been classified as a member of the sucrose nonfermenting-1(SNF-1) family of protein kinases (Barker et al. 1996). SNF-1 represents a primary target of the glucose repression pathway in budding yeast, and glucose repression of metabolism involves a signal transduction pathway that links perception of glucose concentration with repression and/or derepression of glucose-repressible genes (Thevelein 1994). For example, down-regulated genes function in gluconeogenesis and respiration while those up-regulated, function in glycolysis and storage carbohydrate breakdown. SNF-1 is integral to this pathway and glucose-repressible genes cannot be switched on in response to glucose deprivation in the absence of SNF-1 activity (Celenza and Carlson 1989, Gancedo 1993). Thus, it is tempting to suggest that avocado mesocarp HMGR is likewise modulated by the effects of carbohydrate concentration and composition on HMGR kinase activity.

In the present paper we describe experiments that were carried out to determine the effect of fruit size on the endogenous iP and ABA concentration and to establish the effects of an altered CK/ABA ratio on symplastic solute transport, mesocarp cell-to-cell communication and plasmodesmata structure/function in developing Hass avocado fruit.

Materials and Methods

Chemicals — [U-^{14}C]Sucrose (23.2 GBq mmol^{-1}) was purchased from Amersham International (Buckinghamshire, U.K.). ABA, iP, and Lucifer Yellow-CH (LYCH) were purchased from Sigma Chemical Co. (St Louis, MO, U.S.A.). Tetrabromofluorescein (eosin) was obtained from BDH Chemicals (Poole, U.K.).

Plant material and application of chemicals — Experiments were conducted during the 1995/1996 and 1996/1997 seasons using eight-year-old trees of avocado (*Persea americana* Mill. cv. Hass) propagated on clonal 'Duke 7' rootstocks in an orchard on Everdon Estate in the KwaZulu-Natal midlands, South Africa. Compounds of interest were formulated in Tween 20 : acetone : water (1:1:8, v/v) to a final concentration of 1 mg ml^{-1} and 20µl of each, or combinations thereof, injected into the pedicel of individual fruits using a Hamilton 7105 syringe (Hamilton Co.,Reno, NV, U.S.A.) 210 d after full bloom, unless otherwise specified. Control fruit were treated with and without Tween

20:acetone : water (1:1:8, v/v). Following injection, wounds were covered with silicone grease and fruit growth allowed to continue until harvest.

Uptake and distribution of eosin and U-[^{14}C]sucrose — Fruit harvested 226 d after full bloom was immediately supplied with either 5 ml of eosin or 0.5 ml of U-[^{14}C]sucrose (2 MBq in distilled water) via the pedicel and incubated for 48 h at room temperature. For analysis of the distribution of eosin, fruit was bisected longitudinally, the stone removed and the two halves photographed. For analysis of the distribution of radioactivity, three 1 g dry weight samples of mesocarp, seed coat and seed from at least three different fruits were extracted in 80% aqueous methanol at 4°C for 24h. Residual tissue was removed by centrifugation and radioactivity in the supernatant determined by liquid scintillation spectrometry.

Electrophysiological measurements and microinjection procedure — Sections (approximately 2.5 cm in length) of tissue from the mesocarp-seed coat interface region of Hass fruit (226 d after full bloom) were placed in 10 mM NaOH-MES buffer (pH 7.2) containing KC1, $MgCl_2$ and $CaCl_2$ (each 0.5 mM), and 125 mM mannitol, and allowed to recover for a minimum of 30 min at 4°C.

All electrophysiological measurements were made using a WPI Duo 773 electrometer (World Precision Instruments, Sarasota, FL, U.S.A.) fitted with high-impedance, active probes. Inner-filamented glass microelectrodes were prepared using 1 mm diameter pipettes (WPI Kwik-Fil K100-F3), which were pulled with a Narishige PB-7 Pipette Puller (Narishige Co., Tokyo, Japan). Tips were routinely between 0.5 and 1 μm in diameter. Microelectrodes were back-filled with LYCH (5% w/v, in 3 M LiCl) and the shank of the microelectrode filled with 3 M LiCl. Micro-electrodes were attached to KC1 half cells filled with 3 M LiCl, coupled to a WPI high impedance probe and attached WPI PM-10 Piezo controller unit, and WPI DC-3 motorised micromanipulator. Observations were made using an Olympus BHW1 erect image UV photomicroscope with fixed stage, and fitted with ultra-long working distance objectives. Once impaled, cell potentials were monitored using the Duo 773 electrometer. Cell potentials of impaled cells were monitored in darkness after inserting a shutter in the light path to prevent UV exposure and damage to the cells. Once membrane potentials had stabilised (at least — 40 mV as prescribed by Farrar et al. 1992 and van Bel et al. 1996) impaled cells were reverse iontophoresed, using pulsed current (—2 to— 30 nA, for 5 to a maximum of 60 s) in order to inject the dye. Impaled, injected cells were either photographed using an Olympus AD PM-10 camera system or the data recorded using a Panasonic CL-WV 350 video camera, connected to a Panasonic NV-SD3 video recorder. Selected images were produced by frame capture at 250 dots per inch.

Digital imaging—Video recordings showing cell-to-cell transport of LYCH were examined and frames of interest captured in digital format. Files were converted to colour images using a five-colour "pseudocolour" palette based on fluorescence intensity of LYCH concentrations, ranging from black (zero), to aquamarine (low), blue (medium), purple (high), and white (highest). The computer-enhanced digitized images enabled easy visualisation of the actual distribution of LYCH within an avocado mesocarp tissue.

Electron microscopy—An extended fixation and embedding protocol was carried out. Cubes, ca. 10x10x5 mm, of tissue were removed from the seed coat-mesocarp interface of fruits harvested 226 d after full bloom, and placed in glass vials containing cold 5% glutaraldehyde in 0.5 M Na-cacodylate buffer. The fixative was replaced hourly

during the course of a day and then left overnight at 4°C. Fixative solution was changed several times the following day before careful dicing of the tissue into pieces (ca. 3x4x2 mm). Over the course of the next two days, tissue was rinsed in 0.5 M Na-cacodylate buffer and then placed in 2% osmium tetroxide in Na-cacodylate buffer overnight. Thereafter, tissue was rinsed and dehydrated slowly in a cold, graded ethanol series followed by two (30 min) changes of propylene oxide and infiltrated and embedded in resin (Spurr 1969). Silver to gold sections were cut with a diamond knife on an LKB Ultrotome III (Bromma, Sweden), and collected on 200 mesh copper grids. Sections were stained in uranyl acetate followed by lead citrate and viewed in a JEOL JEM 1210 transmission electron microscope (JEOL, Tokyo, Japan) at 80 or 100 kV.

Determination of endogenous ABA and iP — ABA was extracted from freeze-dried mesocarp tissue of fruit harvested 226 d after full bloom and analyzed as previously described (Cowan et al. 1997).

For determination of iP concentration, sub-samples from the same freeze-dried tissue used to quantify ABA, were homogenized in ice-cold 80% methanol containing butylated hydroxytoluene (50 mg liter $^{-1}$) and radiolabeled iP (to correct for losses) in the presence of insoluble polyvinylpyrrolidone (10% w/w). Samples were allowed to extract in darkness at 2°C for 12 h prior to removal of the tissue debris by centrifugation at 10,000 x g for 10 min. The supernatant was reduced to an aqueous volume, acidified to pH 3.0 with acetic acid and applied to a preconditioned $C_{,18}$ Sep-pak cartridge (Millipore, Waters Chromatography, Milford, MA, U.S.A.). The cartridge was washed with 2 ml 50% methanol and iP eluted with 2 ml 80% methanol. Aliquots of the 80% methanol fraction were then used to quantify iP by radioimmunoassay using the procedure developed by Cutting (1991), adapted from Weiler (1980).

Results

Fruit size and endogenous ABA and iP concentration —To determine the relationship between changes in the iP/ABA ratio and appearance of the Hass avocado small-fruit variant, two approaches were adopted. Firstly, we measured the iP and ABA concentration of similarly aged fruit at maturity in an attempt to correlate endogenous iP and ABA concentration, with fruit size. Secondly, a single 20 µg dose of ABA was administered via the pedicel to "normal" fruit (55 d after full bloom) in the linear phase of rapid growth, either in the presence or absence of iP, and the effect of each treatment compared with respect to untreated control and small fruit at time of harvest (226 d after full bloom). The results presented in Figure 1A show that the concentration of iP increased linearly (r^2=0.79) with an increase in fruit size whereas the endogenous ABA concentration was strongly negatively correlated (r^2=0.85). Calculation of the iP/ABA ratio revealed a positive correlation between this ratio and fruit size with a coefficient of linearity of 0.76. Application of ABA to fruit during the linear phase of rapid growth caused fruit growth to slow and induced seed coat senescence (Fig. 1B). When ABA was co-injected with an equal concentration of iP the deleterious effects of ABA were negated, supporting the suggestion that an imbalance in the CK/ABA ratio may be pivotal in the initiation of seed coat senescence and retardation of fruit growth.

Pattern of solute allocation and effect of ABA and/or iP on distribution of radioactivity in fruit pulsed with [^{14}C]sucrose — The pattern of solute movement into

avocado was established by supplying eosin and [^{14}C]sucrose to harvested fruit via the pedicel and monitoring the distribution of eosin in the whole fruit and by determining the allocation of [^{14}C]-label to seed, seed coat and mesocarp tissue. The distribution of eosin is illustrated in Figure 2A. Eosin, which does not permeate plasma membranes, was restricted to the vasculature, which ramifies the mesocarp and coalesces at the chalaza, i.e. the basal region of the fruit. From the chalazal region, eosin distributed in the seed coat tissue along the vascular traces. No lateral diffusion of eosin from the vascular traces in either mesocarp or seed coat tissue was observed.

A more detailed examination of this path and the effect of ABA and iP on solute movement was made by monitoring the accumulation of radioactivity, from pulsed [^{14}C]sucrose, in seed, seed coat and mesocarp tissue. As shown in Figure 2B, the distribution of accumulated radioactivity was essentially similar for untreated, control, iP treated fruit and fruit co-treated with equal amounts of ABA plus iP. Interestingly, the bulk of radioactivity was associated with the seed coat tissue in all treatments. Both the small fruit variant and ABA-treated fruit preferentially accumulated radioactivity in the seed, suggesting that the path via the seed coat was similarly affected in ABA-treated and small-fruit. The pattern of distribution of radioactivity in ABA plus iP-treated fruit was similar to that of the control suggesting that co-treatment with iP negated the deleterious effects of ABA. The relatively high proportion of radioactivity in mesocarp of small fruit and ABA-treated fruit probably reflects reduced solute transport, which is supported by the observation that uptake of [^{14}C]sucrose by these fruit was less than 10% that of the control, in which a 100% uptake occurred.

Membrane potential of seed coat and mesocarp parenchyma of fruit treated with ABA and/or iP — In attempting to define the cellular pathway of postphloem sugar transportin developing avocado fruit the E_m of seed coat and mesocarp parenchyma cells was determined. Although measurement of E_m is difficult (van Bel and Kempers 1990), with due precaution cells were successfully impaled and after sealing of the plasma membrane (indicated by voltage stabilization) values were recorded and these are shown in Table 1. It is evident that an electrical potential gradient exists between seed coat and mesocarp parenchyma and that this gradient was maintained in fruit injected with iP. However, in response to exogenous ABA the gradient was flattened suggesting reduced, or cessation of, solute transport from seed coat to mesocarp tissue. Interestingly, co-injection of ABA plus iP did not restore the E_m gradient between seed coat and mesocarp tissue.

Iontophoresis of LYCH in mesocarp of fruit treated with ABA and/or iP — As shown in Figure 3, false-colour image analysis of LYCH fluorescence showed radial diffusion of the bulk of the dye from injected cells by 2 min indicating a high degree of symplastic connectivity. Similar observations were made for seed coat tissue (data not shown) in which radial diffusion of LYCH was extremely rapid.

Mesocarp cell-to-cell communication in tissue from fruit that had been injected with iP was not affected, as depicted by the pseudocolour images presented in Figure 3A. By comparison, mesocarp cell-to-cell transfer in tissue from fruit pre-treated with ABA was significantly retarded and LYCH was contained within the injected cell for periods in excess of 6 min and in some experiments, beyond 20 min (Fig. 3B). Cell-to-cell communication in mesocarp from fruit treated with iP plus ABA was rapid (Fig. 3C) and resembled that observed in control (Fig. 3D) and iP treated tissue (Fig. 3A).

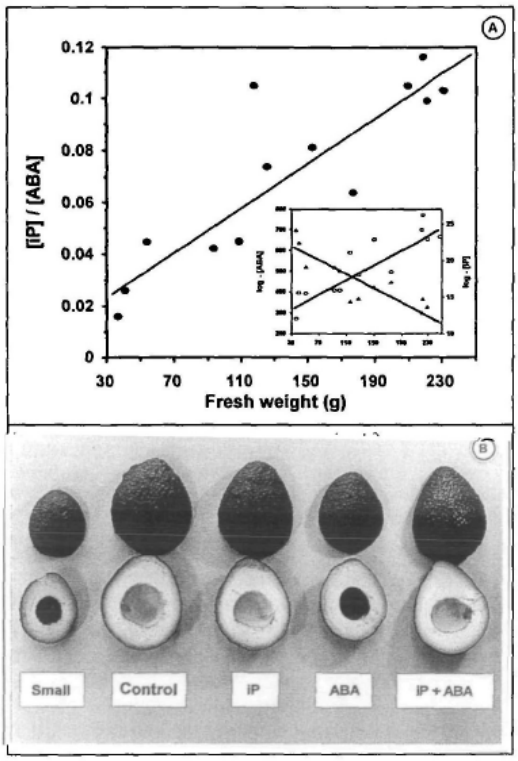

Fig. 1 Relationship between iP and ABA concentration and the Hass avocado small-fruit variant. (A) Mesocarp iP (○) and ABA (▲) content (μg (g DW)$^{-1}$) of fruit harvested 226 d after full bloom expressed as a function of fruit size (fresh weight of whole fruit). ABA and iP were quantified as described in the Materials and Methods. Inset: correlation between $\log_{[ABA]}$ and $\log_{[iP]}$ and fruit size of Hass avocado. (B) ABA induction of the Hass small-fruit phenotype and prevention of this phenomenon by co-injection of ABA with iP. Aliquots of Tween 20 : acetone : water (1 : 1 : 8, v/v) containing 20 μg of ABA, iP, ABA plus iP, were injected via the pedicel 55 d after full bloom and the fruit harvested 226 d after full bloom.

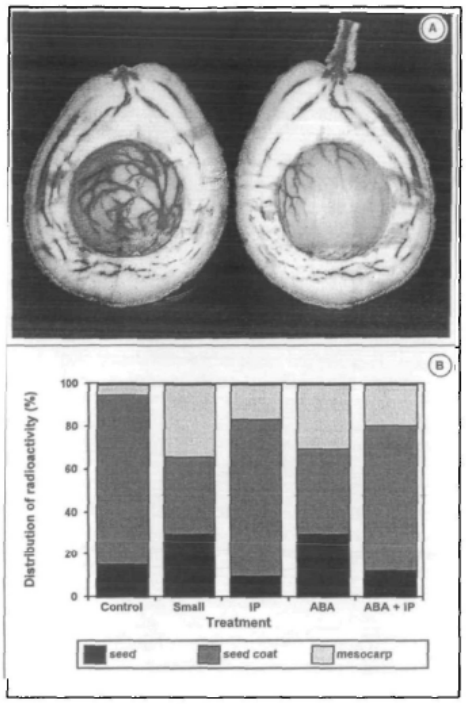

Fig. 2 Pattern of solute movement in Hass avocado fruit and the effect of the small-fruit variant and ABA and iP on solute allocation. (A) Longitudinal section of a detached control fruit harvested 226 d after full bloom and supplied with eosin via the pedicel for 48 h illustrating mesocarp and seed coat vasculature. (B) Distribution of radioactivity in mesocarp, seed coat and seed of small fruit and fruit injected with or without ABA, iP, and ABA plus iP after pulsed labelling with [^{14}C]-sucrose (2 Mbq in distilled water). Tissue was freeze-dried and 1 g dry weight samples extracted in 80% methanol at 4°C for 24 h. After removal of tissue debris, radioactivity was determined by liquid scintillation spectrometry. Data are the mean of three independent studies.

Table 1 Plasma membrane electrical potentials of tissues of developing Hass avocado fruit pre-treated in vivo with or without ABA, iP and ABA plus iP[a]

Treatment	Membrane potential (E_m) in Mv		
	Seed coat Parenchyma	Mesocarp parenchyma	Difference
Control	-44 ± 7 (9)	-56 ± 6 (8)	12
iP	-46 ± 5 (11)	-61 ± 7 (3)	15
ABA	-45 ± 5 (8)	-47 ± 5 (8)	2
iP + ABA	-45 ± 8 (11)	-48 ± 6 (7)	3

[a] Batches of fruit (eight per treatment) were injected via the pedicel with 20//I solutions of Tween 20 : acetone : water (1 : 1 :8, v/v) containing ABA, iP and ABA plus iP (all 1µg µl^{-1}) 210 d after full bloom. Fruit was harvested 16 d later and the plasma membrane electrical potential of mesocarp and seed coat parenchyma cells determined as described in Materials and Methods. Data are the mean±SE. Number of E_m measurements in brackets.

Plasmodesmatal structure/function in developing fruit treated with ABA and/or iP — The principal results of plasmodesmatal ultrastructure in developing Hass avocado fruit pre-treated with or without iP, ABA, and iP plus ABA are illustrated in Figures 4 to 6.

Electron microscope examination of mesocarp tissue from untreated "normal" fruit revealed a highly convoluted plasma membrane, the presence of branched and unbranched plasmodesmatal aggregates within primary pitfields and associated endoplasmic reticulum (Fig.4A). Longitudinal (Fig. 4B) and transverse views (Fig. 4C) showed that these plasmodesmata contained a clearly defined desmotubule surrounding a cytoplasmic annulus of variable electron density. All plasmodesmata appeared to have slightly constricted outer plasmodesmatal orifices that are possibly neck constrictions (Gunning 1975). In many cases, and as shown in Figures 4A and B, the plasmodesmata were associated with large, complex-structured median cavities and appeared branched on one side only (Fig. 4B). Similar analysis of tissues from phenotypically small fruit revealed that mesocarp plasmodesmata were occluded by electron dense material (Fig.4D). There was also evidence of deposition of extra-plasmodesmal material (Fig. 4E) indicative of plasmodesmatal gating in the small fruit variant.

Figure 5 shows that similar structural changes were manifest in sections prepared from mesocarp of ABA-treated fruit. The plasma membrane, as illustrated in Figure 5A and 5B, lacked the highly convoluted appearance evident in untreated tissue (cf. Fig. 4A, B). Furthermore, most plasmodesmata appear to be 'gated'/'plugged' or constricted by a granular electron-dense substance (darts, Fig. 5A) which, when viewed in transverse, forms a collar-like structure on the outer surface (paired arrows, Fig. 5C, E). The complexity of median cavities in avocado mesocarp tissue is again apparent, indicating a high degree of inter-connectivity. Similar observations were made for seed coat tissue from ABA-injected fruit (Fig. 5D). In addition, ABA treatment resulted in highly vesiculate material in an otherwise degenerating seed coat parenchyma cell cytoplasm, typical of the symptoms of advanced senescence.

Figure 6 shows plasmodesmata from the tangential wall of mesocarp cells from iP plus ABA and iP-treated avocado fruit. As illustrated in Figure 6A, the plasmodesmata appear to be occluded by globular electron-dense material at the plasmodesmatal orifices (arrows, Fig. 6A) and the associated plasma membrane lacks the characteristic convoluted appearance. In contrast, plasmodesmata in the neighbouring cell show no evidence of occlusion, the absence of neck constrictions, and the plasma membrane has retained its convoluted appearance (Fig. 6A). Likewise, the plasma membrane is highly convoluted and plasmodesmata appear less electron-dense in tissue from iP-injected fruit than those in untreated tissue and are complex, cross-linked and multi-branched in appearance (Fig. 6B). Plasmodesmata from mesocarp of iP-injected fruit do not appear to be constricted. A striking feature of iP-treated avocado tissues are the large, electron-dense regions, possibly coalesced plasmodesmata, which occur within otherwise normal-looking plasmodesmatal pitfields. Outer wall regions appear more electron-lucent than in control tissues (darts, Fig.6A, B).

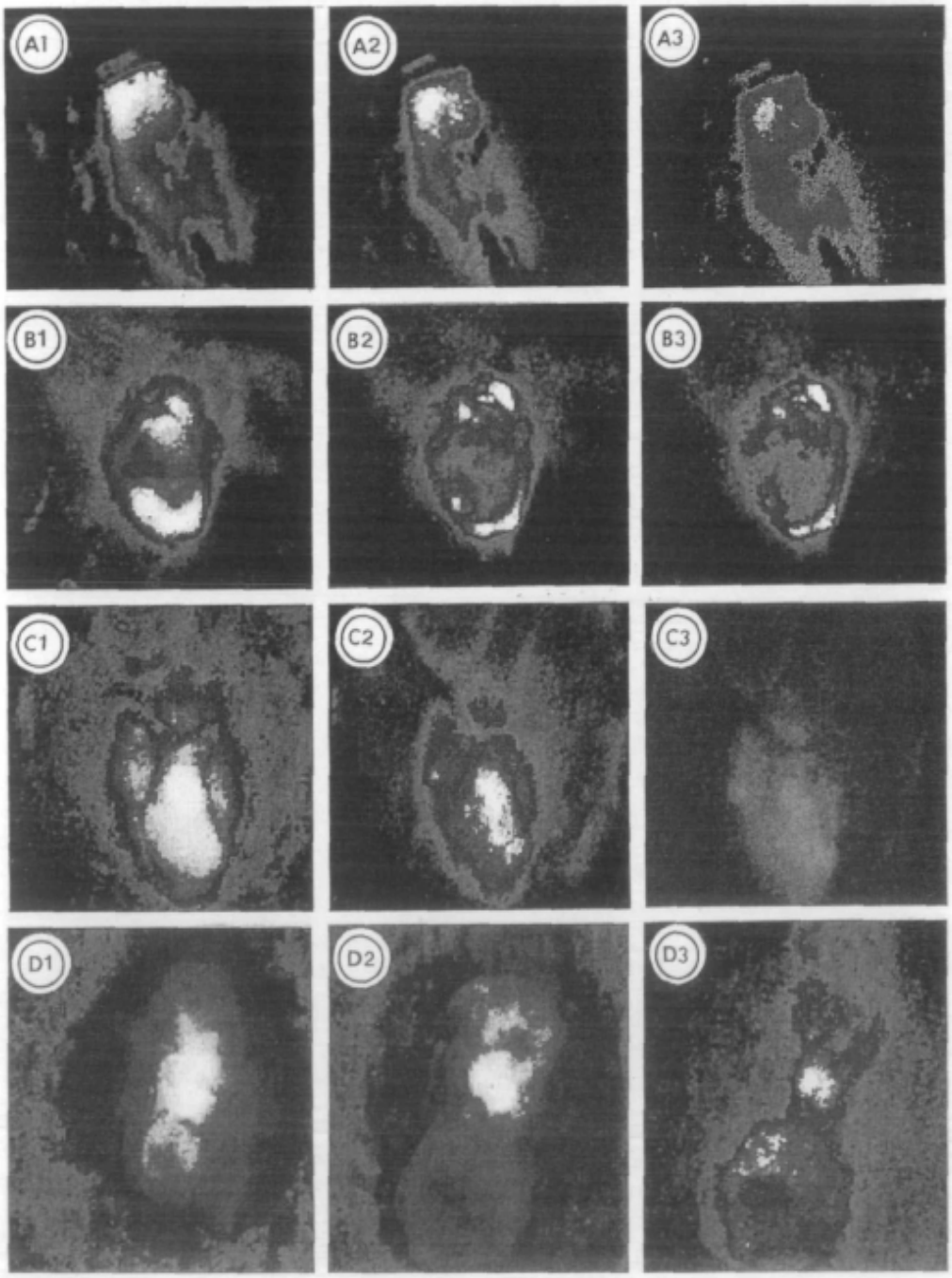

Fig. 3 Microiontophoresis of LYCH in mesocarp parenchyma of 226 day-old Hass avocado fruits pre-treated with or without either ABA and/or iP 210 d after full bloom as described in Table 1. Digitized images of fluorescence micropgraphs of mesocarp from fruit injected with iP and microiontophoresed with LYCH immediately (A1), 1 min (A2) and 2 min (A3) after injection. Digitized images of fluorescence micrographs of mesocarp parenchyma from fruit injected with ABA, microiontophoresed with LYCH, immediately (B1), 2 min (B2) and 6 min (B3) after injection. Digitized images of fluorescence micrographs of mesocarp parenchyma from fruit injected with ABA plus iP and microiontophoresed with LYCH immediately (C1), 1 min (C2) and 2 min (C3) after injection. Digitized images of fluorescence micrographs of hand-cut sections of mesocarp from control fruit microiontophoresed with LYCH immediately (D1), 1 min (D2) and 2 min (D3) after time of injection. A five-colour "pseudocolour palette based on fluorescence intensity of LYCH concentrations, ranging from black (zero), to aquamarine (low), blue (medium), purple (high), and white (highest), was applied.

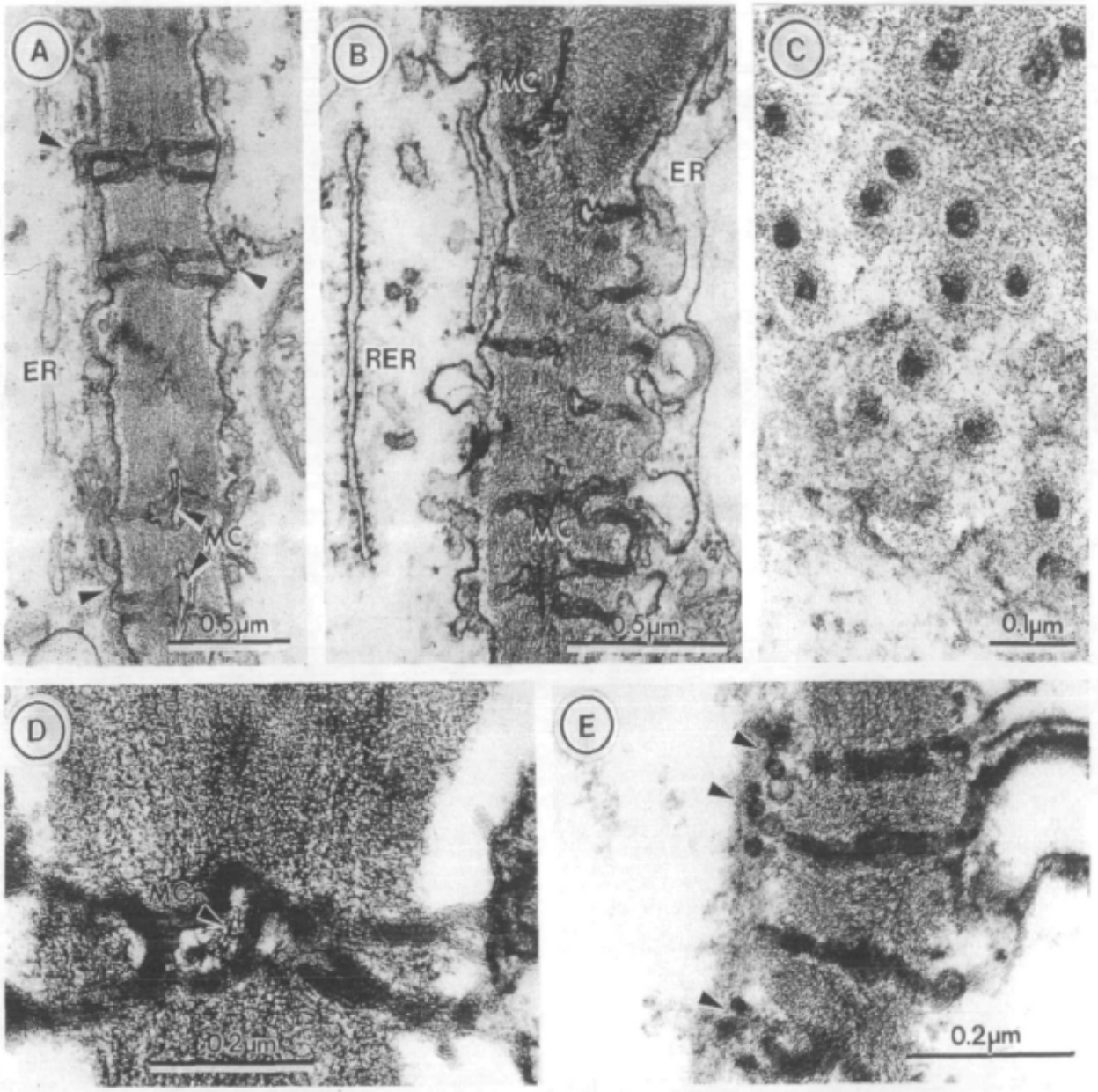

Fig. 4 Ultrastructure of avocado mesocarp plasmodesmata. (A) Transection through the tangential wall between two mesocarp cells, showing mostly branched plasmodesmata, associated with large median cavities (MC) in the middle lamella. Note the close conformation between the endoplasmic reticulum (ER) and the outer orifice of the plasmodesmata (darts). (B) Transection of a common radial wall between two mesocarp cells, but close to the mesocarp-seed coat interface. Unbranched and branched plasmodesmata, associated with ER and rough ER (RER) and MC, occur commonly within these cells. (C) Transection through part of a plasmodesmatal pit field in the radial wall of an inner mesocarp cell. Note the tight conformational structure of the plasmodesmata and the desmotubule with central rod. Most plasmodesmata have an electron-lucent cytoplasmic sleeve in these sections. Longitudinal (D and E) sections of plasmodesmata from mesocarp tissue of the small fruit variant. Note, electron-dense material within branched plasmodesma and associated MC and extra-plasmodesmal material which is deposited (arrowheads) to form cap-like structures which occlude the plasmodesmata.

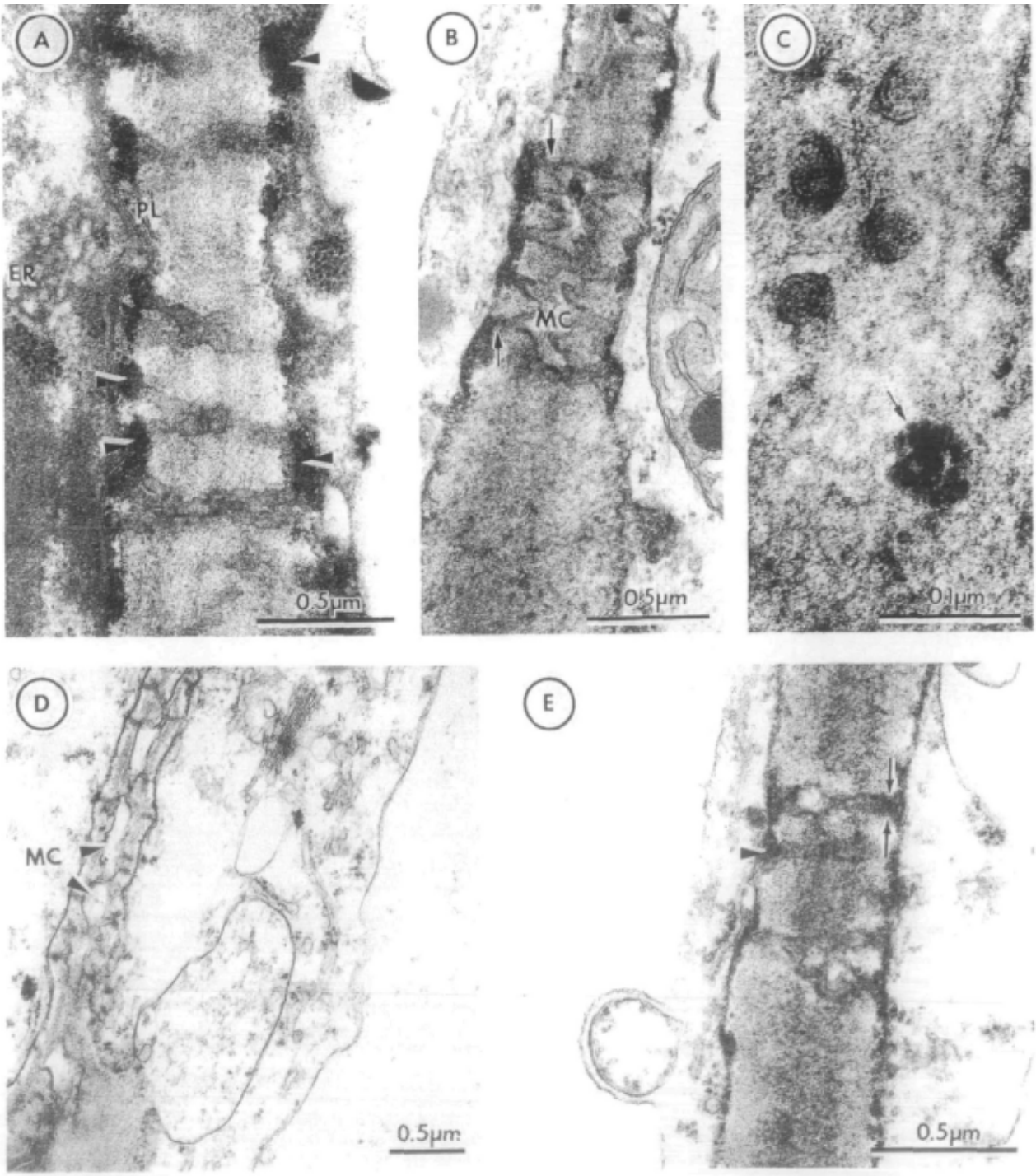

Fig. 5 Ultrastructure of plasmodesmata in ABA-injected Hass avocado fruit. (A) Transection of a tangential wall between mesocarp cells. Note, unbranched and branched plasmodesmata associated with endoplasmic reticulum (ER) are all occluded by granular electron-dense material deposited in or near the plasma membrane (PL) gating the outer orifice (darts). (B) Transection of a more deeply-seated mesocarp cell. Note, complex median cavities (MC) which interconnect the plasmodesmata. As in (A), all plasmodesmata are gated by electron-dense material which appears to form a tight collar (arrows). (C) Transection through part of a plasmodesmatal pit field in the radial wall of an inner mesocarp cell. Note the tight conformational structure of the plasmodesmata and the desmotubule with central rod (arrow). Most plasmodesmata have an electron-lucent cytoplasmic sleeve in these sections. (D) Transection through a common tangential wall area between two seed coat cells. Note large MC between plasmodesmata (darts). Cytoplasm within these seed coat cells appears degenerate and possibly senescent. (E) Shows the radial wall between two seed coat cells. Plasmodesmata are gated (dart) as in Figs. 5A and B and there is clear evidence for neck constrictions (arrows).

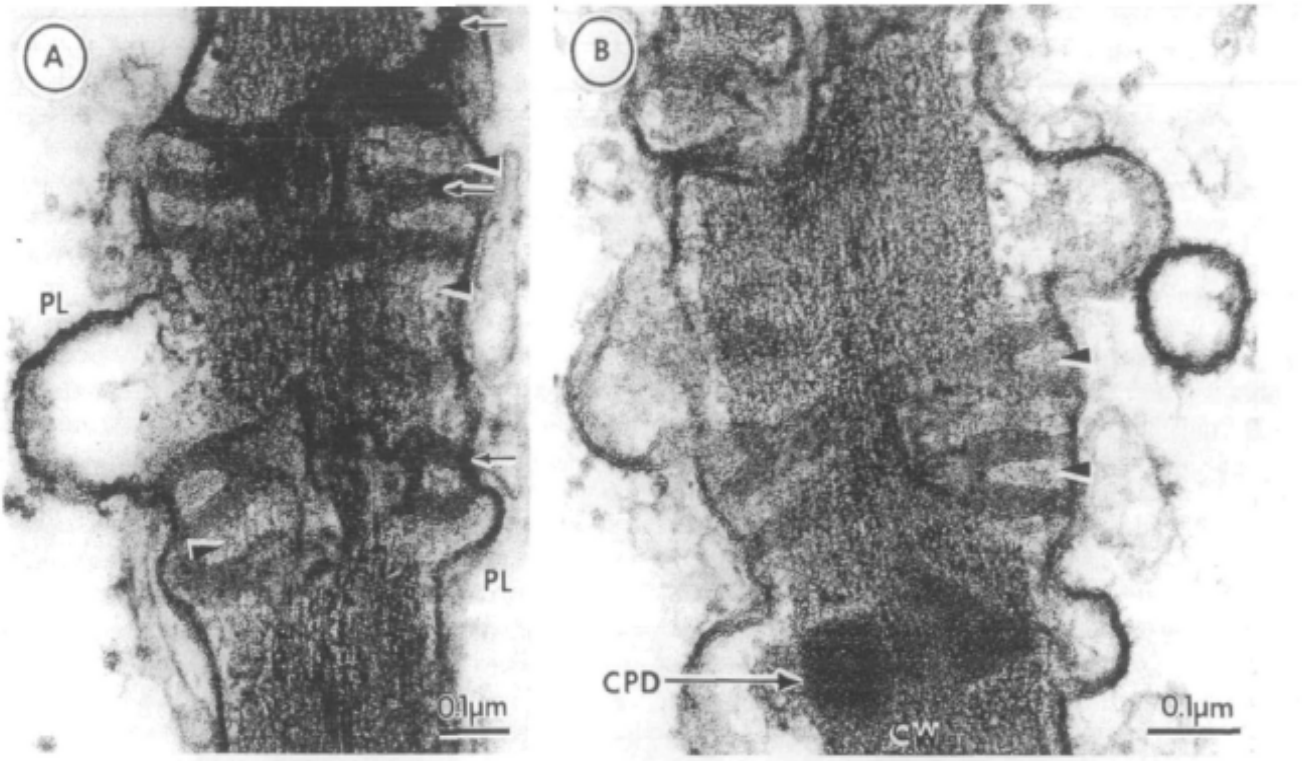

Fig. 6 Ultrastructure of plasmodesmata in iP plus ABA and iP-injected Hass avocado fruit. (A) Transection showing common wall between two mesocarp cells, in iP plus ABA-treated fruit. Note the convoluted plasma membrane (PL), electron-lucent outer wall (darts) and electron-dense material (arrows) which occludes some of the plasmodesmata. (B) Transection of a common tangential wall between two mesocarp cells in iP-injected fruit. Note complex cross-linked multi-branched plasmodesmata in this tissue. Plasmodesmata are separated by an electron-lucent wall region (darts). Commonly and of interest, are the large electron-dense possibly, coalesced plasmodesmata (CPD) in the cell wall (CW).

Discussion

ABA and hass avocado fruit size — Results from the present investigation provide good evidence to support an interaction between avocado fruit ABA concentration and appearance of the Hass small-fruit variant. Mesocarp ABA concentration of mature fruit was negatively correlated to fruit size and application of ABA during the linear phase of rapid growth caused seed coat senescence and retarded fruit growth.

The ability of ABA to induce the Hass small fruit variant at all stages of fruit growth (Fig. 1; Cowan et al. 1997) suggests that endogenous ABA concentration is a major contributing factor. Several studies have revealed that the ABA content of young fruit is high and declines during the course of development (Fraser et al. 1995, Guinn 1982). Likewise, the ABA concentration of developing Hass fruit is initially high and declines with increasing fruit age (Cowan et al. 1997). Although the physiological significance of elevated ABA levels during the initial stages of fruit growth remains unresolved, there is evidence to support a role for ABA in photosynthate unloading from phloem in developing grains, seeds and fleshy fruits. For example, application of ABA to wheat and barley grains promoted import of recently fixed photoassimilate (Dewdney and McWha 1979, Tietz et al. 1981). Furthermore, Schiissler et al. (1984) demonstrated

that testa of large seeded genotypes of soybean had higher ABA content than small-seeded genotypes and suggested that the additional ABA acted to increase sieve element unloading into the testa apoplast. Likewise, ABA enhanced the uptake of sugar into, vacuoles of apple fruit flesh (Beruter 1983, Yamaki and Asakura 1991), sugar beet root tissue discs (Saftner and Wyse 1984) and increased the sugar content of developing citrus fruit (Kojima et al. 1995).

ABA and iP, and symplastic solute transport — The distribution of radioactivity in small Hass fruit and fruit pre-treated with ABA, following pulsed application of [^{14}C]sucrose, was similar. Thus, when compared to untreated and iP-treated fruit, incorporation of label into seed coat tissue was reduced by 50% whereas the amount of [^{14}C] associated with the seed increased two-fold. Measurement of seed coat and mesocarp E_m revealed an electrical potential gradient between seed coat and mesocarp tissue that was abolished in tissue from fruit pre-treated with ABA. Furthermore, microiontophoretic and detailed ultrastructural studies of mesocarp and seed coat tissue revealed that plasmodesmata in ABA-treated fruit were 'plugged' by electron dense material deposited at the annuli, a phenomenon that was negated by co-injection of fruit with iP. Although the pattern of [^{14}C] allocation from pulsed [^{14}C]sucrose, and cell-to-cell transport of LYCH were similar for mesocarp of control fruit and fruit pre-treated with iP and iP plus ABA, co-injection of iP with ABA did not reverse the apparent ABA-induced membrane depolarization of mesocarp parenchyma suggesting operation of a second, plasma membrane-localized pathway, that is unaffected by iP but sensitive to ABA.

Hartung et al. (1980) demonstrated that ABA caused plasmamembrane hyper-polarization in the short term, increased soluble sugar content (measured as glucose units) and reduced glucose-induced changes in membrane potential in *Lemna gibba*. These authors suggested that stimulation of invertase activity could have caused the increase in glucose concentration.

ABA is purported to stimulate soluble acid invertase activity, at least in developing soybean seeds (Ackerson 1985). Activity of this enzyme is thought to increase the sucrose gradient between source and sink tissue to facilitate phloem unloading (Ruffner et al. 1990). Several studies have revealed that increased expression of extracellular acid invertase reduces plant organ growth (Dickinson et al. 1991, Heineke et al. 1992, von Schaewen et al. 1990), whereas Klann et al. (1996) showed that expression of an antisense soluble acid invertase in tomato results in sucrose accumulation, decreased hexose sugar concentration and reduced fruit size. We have observed that insoluble acid invertase activity of avocado seed tissue is substantially higher in the small-fruit variant and that mesocarp soluble and insoluble acid invertase activity in the small fruit is reduced (R.F. Cripps, E.W. Richings and A.K. Cowan, unpublished data). In addition, while seed and seed coat sucrose concentration was reduced in small fruit, total hexose concentration was similar, although glucose accumulated in the seed and fructose in the mesocarp (E.W. Richings and A.K. Cowan, unpublished data). Together, these observations suggest a change in the sucrose gradient between seed coat, and seed and mesocarp tissue in small fruit. Since symplastic continuity in both seed coat and mesocarp tissue is arrested and the E_m gradient between seed coat and mesocarp parenchyma is abolished in normal fruit by ABA treatment and in the small-fruit variant, it is suggested that the seed assumes dominance over the mesocarp for available sugar in the absence of a functional seed coat. Whilst

measurements of E_m obtained using avocado tissues were not high, it must be remembered that mature, pre-climacteric fruit tissue was used in the present study which would not be expected to yield high values such as those obtained in leaf mesophyll cells (van Bel et al. 1996). Nevertheless, it is generally accepted that the more negative E_m becomes, the more physiologically active cells are assumed to be in terms of cell-to-cell transport. Thus, our results appear to indicate that seed coat and mesocarp tissue are within the same electrophysiological (and by implication, structurally-connected) continuum. Taken together, these results suggest that bulk solute movement into developing avocado fruit occurs along the path: pedicel vasculature →mesocarp vasculature → chalaza → seed and/or seed coat vasculature→ mesocarp.

Plasmodesmatal structure/function in response to ABA and iP — Analysis of Hass avocado mesocarp and seed coat plasmodesmatal ultrastructure revealed three distinct changes induced by expression of the small fruit phenotype and injection of fruit with ABA that were absent in normal fruit and fruit injected with ABA plus iP. Firstly, median cavities were clearly evident in continuous branched plasmodesmata in control and iP-treated fruit. As depicted in Figures 4, 5 and 6, plasmodesmatal branching was reduced in phenotypically small fruit and in fruit that had been pre-treated with ABA whereas this effect was absent in fruit injected with ABA plus iP. A correlation between arrested branched plasmodesmatal development and onset of accelerated senescence has been established for leaf tissue (Ding et al. 1993). Thus emergence of the Hass small fruit variant, which is associated with early senescence of the seed coat, implies that development and structure/function of plasmodesmata may be crucial in the determination of final fruit size. Since primary plasmodesmata are formed cytokinetically during cell plate assembly and secondary plasmodesmata arise de novo, post-cytokinesis, in pre-existing cell walls (Lucas et al. 1993), we conclude that avocado mesocarp and seed coat plasmodesmata are morphological modifications of simple primary plasmodesmata. As stated by Ehlers and Kollmann (1996), primary plasmodesmata may undergo morphological change but will not develop into plasmodesmata of a truly secondary origin. Whether CKs play a role in mediating branching of primary plasmodesmata is currently unknown.

Secondly, our data illustrate the presence of electron-dense, particulate material associated with the neck region of plasmodesmata in mesocarp and seed coat tissue of small fruit, and ABA- and ABA plus iP-treated avocado fruit. Coupled with microiontophoretic analysis, these data suggest that application of ABA blocked plasmodesmatal molecular trafficking by inducing deposition of globular plasmodesmatal-localized material. The absence of this material in control and iP-treated tissues, as well as its apparent reduction in ABA plus iP-treated material, suggests that it was formed in response to elevated ABA.

It is essential that plasmodesmata are dynamic to accommodate larger or smaller trafficked molecules in cell-to-cell chemical communication. Robards and Lucas (1990) suggest that up- or down-regulation of plasmodesmatal pore size is achieved by either modification of the central lipoprotein core or, by deposition of callose near the cytoplasmic annulus. Since the latter mechanism does not appear to be involved in the fine regulation of plasmodesmata calcium binding proteins and contractile proteins (e.g. centrin) have also been considered as candidates to fulfil a regulatory role in the control of plasmodemata (Overall and Blackman 1996). As suggested by Morris (1996) a

requirement for components of signal transduction pathways in the activation of these proteins, may implicate the involvement of phytohormone agonists. Thus, and in view of the data presented in this paper, a central role for ABA in the regulation of plasmodesmatal pore diameter, as a means of either controlling or curtailing molecular trafficking in developing avocado fruit seems very plausible. Since integrity of the seed coat and associated mesocarp is essential for maintenance of sink strength throughout fruit development, ABA-induced down-regulation of plasmodesmatal pore size may contribute to early seed coat senescence and cessation of fruit growth.

Finally, the plasma membrane adjacent to primary pitfields appears highly convoluted in mesocarp from control and iP-treated fruit. In contrast, the plasma membrane in mesocarp cells of the small fruit variant and fruit pretreated with ABA lacked this convoluted appearance suggesting ABA-induced diminution of membrane activity. A similar response was observed in seed coat tissue. Interestingly, injection of fruit with ABA plus iP negated this effect apparently only on one side of the plasma membrane/cell wall complex of adjacent cells, i.e. opposite occluded plasmodesmata. Although the physiological significance of this observation has yet to be established, it does suggest that ABA treatment affected both symplastic and apoplastic solute movement in avocado fruit.

Carbohydrate-modulation of development is thought to involve a hexose sensor comprising phosphorylated glucose and fructose and a putative plasma membrane (plasmodesmatal?) signal (Koch 1996). The concentration of each component is determined by the mechanism of sugar uptake. For example, hydrolysis of symplastically imported sucrose by soluble invertase generates more substrate for the hexose sensor than does sucrose synthase whereas uptake of sugar, hydrolysed extracellularly, requires an energy-coupled plasma membrane hexose carrier that may be sterol-modulated (Grandmougin-Ferjani et al. 1997) and ABA-sensitive. Availability of carbohydrate might also impact on plasmodesmatal pore size to promote pathway switching from symplastic to apoplastic transfer. Tentative evidence in support of this phenomenon has recently been obtained from studies of the pathway of postphloem sugar transport in developing tomato fruit (Patrick and Offler 1996, Ruan and Patrick 1995). Results from the present investigation therefore suggest that sugar transport pathway switching in Hass avocado may be a response to altered CK/ABA ratio and that accumulation of ABA arrests both symplastic and apoplastic sugar transport causing seed coat senescence, loss of sink strength and reduced fruit growth. Even so, the complexity of expression of the Hass small fruit phenotype and the potential role of ABA in this process indicates operation of multiple signalling pathways that are influenced by hormone balance and sugar concentration and composition.

This research was supported by grants from the Foundation for Research Development, South African Avocado Growers' Association and the University of Natal. Everdon Estate is acknowledged for providing access to experimental orchards. The assistance by staff of the Electron Microscopy Unit, University of Natal Pietermaritzburg in gratefully acknowledged.

References

Ackerson, R.C. (1985) Invertase activity and abscisic acid in relation to carbohydrate status in developing soybean reproductive structures. *Crop Sci.* 25: 615-618.

Bach, T. J. and Lichtenthaler, H.K. (1983) Inhibition by mevinolin of plant growth, sterol

formation and pigment accumulation. *Physiol. Plant.* 59: 50-60.
Ballard, L.A.T. and Wildman, S.G. (1963) Induction of mitosis by sucrose in excised and attached dormant buds of sunflower *(Helianthus annuus* L.) *Aust. J. Biol. Sci.* 17: 36-43.
Barker, J.H.A., Slocombe, S.P., Ball, K.L., Hardie, D.G., Shewry, P.R. and Halford, N.G. (1996) Evidence that barley 3-hydroxy-3-methylglutaryl-coenzyme A reductase kinase is a member of the sucrose nonfermenting-1 -related protein kinase family. *Plant Physiol.* 112: 1141-1149.
Beruter, J. (1983) Effects of abscisic acid on sorbitol uptake in growing apple fruits. *J. Exp. Bot.* 34: 737-743.
Blanke, M.M. and Lenz, F. (1989) Fruit photosynthesis. *Plant Cell Environ.* 12: 31-46.
Blanke, M.M. and Whiley, A.W. (1995) Bioenergetics, respiration cost and water relations of developing avocado fruit. /. *Plant Physiol.* 145: 87- 92.
Brooker, J.D. and Russell, V.W. (1979) Regulation of microsomal 3-hydroxy-3-methylglutaryl coenzyme A reductase from pea seedlings: rapid post-translational phytochrome-mediated decrease in activity and in vivo regulation by isoprenoid products. *Arch. Biochem. Biophys.* 198: 323-334.
Celenza, J.H. and Carlson, M. (1989) Mutational analysis of the *Saccharomyces cerevisiae* SNF1 protein kinase and evidence for functional interaction with the SNF4 protein. *Mol. Cell Biol.* 9: 5034-5044.
Coombe, B.G. (1976) The development of fleshy fruits. *Annu. Rev. Plant Physiol.* 27: 207-228.
Cowan, A.K., Moore-Gordon, C.S., Bertling, I. and Wolstenholme, B.N. (1997) Metabolic control of avocado fruit growth: isoprenoid growth regulators and the reaction catalysed by 3-hydroxy-3-methylglutaryl coenzyme A reductase. *Plant Physiol.* 114: 511-518.
Cutting, J.G.M. (1991) Determination of the cytokinin complement in healthy and witchesbroom malformed proteas. / . *Plant Growth Regul.* 10: 85-89.
Dewdney, S.J. and McWha, J.A. (1978) The metabolism and transport of abscisic acid during grain fill in wheat. *J. Exp. Bot.* 29: 1299-1308.
Dickinson, CD., Altabella, T. and Chrispeels, M.J. (1991) Slow-growth phenotype of transgenic tomato expressing apoplastic invertase. *Plant Physiol.* 95: 420-425.
Ding, B., Haudenshield, J.S., Willmitzer, L. and Lucas, W.J. (1993) Correlation between arrested secondary plasmodesmal development and onset of accelerated leaf senescence in yeast acid invertase transgenic tobacco plants. *Plant J.* 4: 179-189.
Ehlers, K. and Kollmann, R. (1996) Formation of branched plasmodesmata in regenerating *Solarium nigrum-piotoplasls. Planta* 199: 126-133.
Farrar, J., van der Schoot, C , Drent, P. and van Bel, A.J.E. (1992) Symplastic transport of Lucifer Yellow in mature leaf blades of barley: potential mesophyll-to-sieve-tube transfer. *New Phytol.* 120: 191-196.
Fraser, P.D., Hedden, P., Cooke, D.T., Bird, C.R., Schuch, W. and Bramley, P.M. (1995) The effect of reduced activity of phytoene synthase on isoprenoid levels in tomato pericarp during fruit development and ripening. *Planta* 196: 321-326.
Gancedo, J.M. (1992) Carbon catabolite repression in yeast. *Eur. J. Biochem.* 206: 297-313.
Grandmougin-Ferjani, A., Schuler-Muller, I. and Hartmann, M. (1997) Sterol modulation

of the plasma membrane H+-ATPase activity from corn roots reconstituted into soybean lipids. *Plant Physiol*. 113: 163-174.
Guinn, G. (1982) Fruit age and changes in abscisic acid content, ethylene production, and abscission rate of cotton fruits. *Plant Physiol*. 69: 349-352.
Gunning, B.E.S. (1975) The role of plasmodesmata in short distance transport to and from the phloem. In Intercellular Communication in Plants. Edited by Gunning, B.E.S and Robards, A.W. pp. 203-227. Springer-Verlag, Berlin.
Hartung, W., Ullrich-Eberius, C.I., Luttge, U., Bocher, M. and Navocky, A. (1980) Effect of abscisic acid on membrane potential and transport of glucose and glycine in *Lemna gibba* Gl. *Planta* 148: 256-261.
Heinke, D., Sonnewald, U., Gunter, G., Leidreiter, K., Wieke, I., Raschke, K., Willmitzer, L. and Heldt, H.W. (1992) Apoplastic expression of a yeast-derived invertase in potato. *Plant Physiol*. 100: 301-308.
Ho, L.C. (1988) Metabolism and compartmentation of imported sugars in sink organs in relation to sink strength. *Annu. Rev. Plant Physiol.* Plant Mol. Biol. 39: 355-378.
Klann, E.M., Chetelat, R.T. and Bennett, A.B. (1993) Expression of acid invertase gene controls sugar composition in tomato (Lycopersicon) fruit. *Plant Physiol*. 103: 863-870.
Klann, E.M., Hall, B. and Bennett, A.B. (1996) Antisense acid invertase (TIV1) gene alters soluble sugar composition and size in transgenic tomato fruit. *Plant Physiol*. 112: 1321-1330.
Koch, K.E. (1996) Carbohydrate-modulated gene expression. Annu. Rev. *Plant Physiol. Plant Mol. Biol*. 47: 509-540.
Koch, K.E., Nolte, K.D., Duke, E.R., McCarty, D.R. and Avigne, W.T. (1992) Sugar levels modulate differential expression of maize sucrose synthase genes. *Plant Cell* 4: 59-69.
Kojima, K., Yamada, Y. and Yamamoto, M. (1995) Effects of abscisic acid injection on sugar and organic acid contents of citrus fruit. *J. Japan. Soc. Hort. Sci*. 64: 17-21.
Kozlowski, T.T. (1992) Carbohydrate sources and sinks in woody plants. *Bot. Rev*. 58: 107-222.
Lucas, W. J., Ding, B. and van der Schoot, C. (1993) Plasmodesmata and the supra-cellular nature of plants. *New Phytol*. 125: 435-476.
Miller, M.E. and Chourey, P.S. (1992) The maize invertase-deficient minature-1 seed mutation is associated with aberant pedicel and endosperm development. *Plant Cell A*: 297-305.
Moore, K.B. and Oishi, K.K. (1994) 3-Hydroxy-3-methylglutaryl CoA reductase activity in the endosperm of maize vivipary mutants. *Plant Physiol*. 105: 119-125.
Morris, D.A. (1996) Hormonal regulation of source-sink relationships: an overview of potential control mechanisms. In Photo Assimilate Distribution in Plants and Crops. Edited by Zamski, E. and Schaffer, A.A. pp. 441-465. Marcel Dekker, New York.
Müller, M.L., Barlow, P.W. and Pilet, P.-E. (1994) Effect of abscisic acid on the cell cycle in the growing maize root. *Planta* 195: 10-16.
Ohyama, A., Ito, H., Sato, T., Nishimura, S., Imai, T. and Hirai, M. (1995) Suppression of acid invertase activity by antisense RNA modifies the sugar composition of tomato fruit. *Plant Cell Physio*l. 36: 369-376.
Overall, R.L. and Blackman, L.M. (1996) A model of the macromolecular structure of

plasmodesmata. *Trends Plant Sci*. 1: 307-311.
Patrick, J.W. (1997) Phloem unloading: sieve element unloading and postsieve element transport. *Annu. Rev. Plant Mol. Biol. Plant Physiol.* 48: 191-222.
Patrick, J.W. and Offler, C.E. (1996) Post-sieve element transport of photoassimilates in sink regions. *J. Exp. Bot.* 47: 1165-1177.
Robards, A.W. and Lucas, W.J. (1990) Plasmodesmata. *Annu. Rev. Plant Physiol. Plant Mol. Biol.* 41: 369-419.
Ruan, Y. and Patrick, J.W. (1995) The cellular pathway of postphloem sugar transport in developing tomato fruit. *Planta* 196: 434-444.
Ruffner, H.P., Alder, S. and Rast, D.M. (1990) Soluble and wall associated forms of invertase in *Vitis vinifera*. *Phytochemistry* 29: 2083-2086.
Russell, D.W. and Davidson, H. (1982) Regulation of cytosolic HMGCoA reductase activity in pea seedlings: contrasting responses to different hormones, and hormone-product interaction, suggest hormonal modulation of activity. *Biochim. Biophys. Res. Commun.* 104: 1537-1543.
Saftner, R.A. and Wyse, R.E. (1984) Effect of plant hormones on sucrose uptake by sugar beet root tissue discs. *Plant Physiol.* 74: 951-955.
Schussler, J.R., Brenner, M.L. and Brfln, W.A. (1984) Abscisic acid and its relationship to seed filling in soybeans. *Plant Physiol.* 76: 301-306.
Spurr, A.R. (1969) A low-viscosity epoxy resin embedding medium for electron microscopy. *J. Ultrastruct. Res.* 26: 31-43.
Steyn, E.M.A., Robertse, P.J. and Smith, D. (1993) An anatomical study of ovary-to-cuke development in consistently low-producing trees of 'Fuerte' avocado (*Persea americana* Mill.) with special reference to seed abortion. *Sex. Plant Reprod*. 6: 87-97.
Thevelein, J.M. (1994) Signal transduction in yeast. *Yeast* 10: 1753-1790.
Thorne, J.H. (1985) Phloem unloading of C and N assimilates in developing seeds. *Annu. Rev. Plant Physiol.* 36: 317-343.
Tietz, A., Ludewig, M., Dingkuhn, M. and Dorffling, K. (1981) Effect of abscisic acid on transport of assimilates in barley. *Planta* 152: 557-561.
van Bel, A.J.E., Hendricks, J.H.M., Boon, E.J.M.C., Gamalei, Y.V.Ph. and Van de Merwe, A. (1996) Different ratios of sucrose/raffinose-induced membrane depolarizations in the mesophyll of species with symplasmic (*Catharanthus roseus*, *Ocimum basilicum*) or apoplasmic (*Impatiens walleriana, Vicia faba*) minor vein configurations. *Planta* 199: 185-192.
van Bel, A.J.E. and Kempers, R. (1990) Symplastic isolation of the sieve element-companion cell complex in the phloem of *Ricinus communis* and *Salix alba* stems. *Planta* 183: 69-76.
von Schaewen, A., Stitt, M., Schmidt, R., Sonnewald, U. and Willmitzer, L. (1990) Expression of a yeast-derived invertase in the cell wall of tobacco and *Arabidopsis* plants leads to accumulation of carbohydrate and inhibition of photosynthesis and strongly influences growth and phenotypic expression of transgenic tobacco plants. *EMBO J*. 9: 3033-3044.
Webster, P.L. and Henry, M. (1987) Sucrose regulation of protein synthesis in pea root meristem cells. *Environ. Exp. Bot*. 27: 253-262.
Weiler, E.W. (1980) Radioimmunoassay for trans-zeatin and related cytokinins. *Planta* 149: 155-162.

Yamaki, S. and Asakura, T. (1991) Stimulation of the uptake of sorbitol into vacuoles from apple fruit flesh by abscisic acid and into protoplasts by indoleacetic acid. *Plant Cell Physiol.* 32: 315-318.
Zilkah, S. and Klein, I. (1987) Growth kinetics and determination of shape and size of small and large avocado fruits cultivar Hass on the tree. *Scientia Hort.* 32: 195-202.
Zinselmeier, C, Westgate, M.E., Schussler, J.R. and Jones, R.J. (1995) Low water potential disrupts carbohydrate metabolism in maize (*Zea mays* L.) ovaries. *Plant Physiol.* 107: 385-391.